KICS The Korean Institute of Communications and Information Sciences

Available online at www.sciencedirect.com
ScienceDirect

ICT Express 8 (2022) 283–289

www.elsevier.com/locate/icte

HADR: A Hybrid Adaptive Data Rate in LoRaWAN for Internet of Things

Arshad Farhad, Jae-Young Pyun*

Wireless and Mobile Communication System Laboratory, Department of Information and Communication Engineering, Chosun University, Gwangju 61452, Republic of Korea

Received 10 September 2021; received in revised form 29 October 2021; accepted 26 December 2021
Available online 3 January 2022

Abstract

Resource allocation (e.g., spreading factor and transmit power) to static and mobile Internet of Things (IoT) applications is significantly challenging. To meet the IoT application requirements, LoRaWAN assigns resources to static and mobile end devices (EDs) using an adaptive data rate (ADR) and blind ADR (BADR), respectively. However, these ADRs are designed for a particular application at a time (e.g., either ADR for static or BADR for mobile EDs). Therefore, to accommodate diverse IoT applications, we propose a novel approach called "hybrid ADR (HADR)" for allocating resources to static and mobile EDs. The proposed HADR finds the ED status (i.e., static or mobile) and executes a proper ADR concerning ED status. Simulation results show that HADR optimally allocates resources to static and mobile EDs simultaneously, which improves the packet success ratio up to 11% and 20% compared to ADR and BADR, respectively.

Keywords: Internet of Things; Adaptive data rate; Blind ADR; Hybrid ADR; LoRa and loRaWAN; Resource allocation

1. Introduction

LoRa defines the physical layer features, employing chirp spread spectrum modulation, which enables long-range and ultra-low energy communication [1]. While long-range wide area network (LoRaWAN) defines an open-source medium access control (MAC) layer protocol developed by the LoRa Alliance, becoming a de-facto technology for the Internet of Things (IoT) owing to its long-range connectivity and low deployment cost [2–4]. Moreover, it provides support for a large number of EDs connectivity through single or multiple gateways (GWs), a network server (NS), and application servers, as shown in Fig. 1. Furthermore, LoRaWAN supports two modes of operations: confirmed and unconfirmed. An ED employing confirmed mode expects an acknowledgment (ACK) from NS, while ACK is not required in the unconfirmed mode [5]. In both communication modes, the ED always allocates its transmission resource with spreading factors (SF $\in$ [7, 8, 9, 10, 11, 12]).

LoRaWAN uses adaptive data rate (ADR) to assign resources, e.g., SF and transmit power (TP), to EDs [6]. When ADR selects the proper SF and TP parameters, the communication between ED and GW is established and maintained for high-capacity and static applications, for instance, metering. In contrast, when the propagation environment changes like the case of mobile IoT applications owing to ED movement, the ADR suffers from significant packet loss and convergence period [7].

On the one hand, to address the issues in ADR, some of the current research works suggested enhancements to the typical ADR under static scenarios [8–11]. [8] presented a modified ADR based on coding rate adaptation and an average of M UL packets (i.e., $M = 20$) received at the NS to improve the energy consumption efficiency and packet success ratio (PSR). In [9], the authors proposed enhanced ADR (EADR) by suggesting the reduction of M (i.e., $M = 5$ was assumed) packets during SF and TP parameter adaptation at the NS side. The proposed EADR in [9] computed the PSR for individual ED involved in communication, and the PSR was compared to a pre-defined threshold (i.e., PSR = 80%). In the case of PSR less than the threshold, NS side ADR transmitted the $LinkADRReq$ MAC command, containing newly identified SF and TP. As the simulation work, in [10,11], SF and TP adjustment approaches were presented, where the NS is responsible for allocating both parameters concerning the SF sensitivity thresholds.

On the other hand, limited attention is given to the resource assignment of EDs under a mobility scenario. [12]

* Corresponding author.
E-mail addresses: arshad@chosun.kr (A. Farhad), jypyun@chosun.ac.kr (J.-Y. Pyun).
Peer review under responsibility of The Korean Institute of Communications and Information Sciences (KICS).

https://doi.org/10.1016/j.icte.2021.12.013

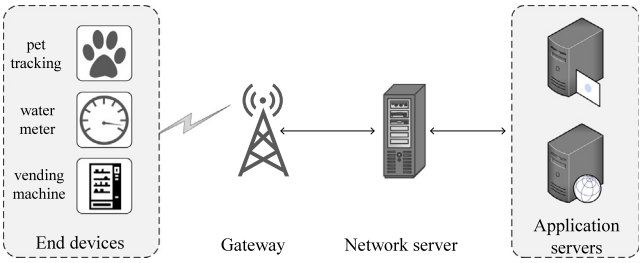

Fig. 1. LoRaWAN star-of-stars architecture.

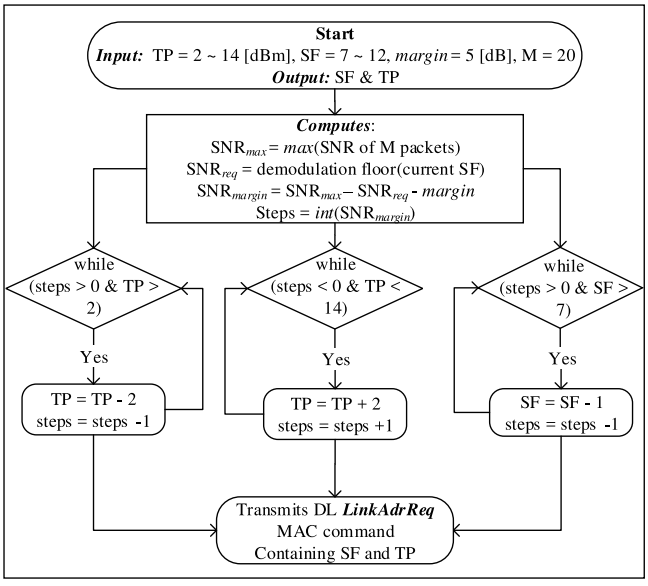

Fig. 2. LoRaWAN adaptive data rate at network server side [11].

Table 1
Sensitivity thresholds and required SNR (SNR_{req}) for 125-kHz mode.

SF	(S_g) [dBm]	(S_e) [dBm]	SNR_{req} [dB]
12	−142.5	−137.0	−20
11	−140.0	−135.0	−17.5
10	−137.5	−133.0	−15
9	−135.0	−130.0	−12.5
8	−132.5	−127.0	−10
7	−130.0	−124.0	−7.5

improved the existing ADR by using the trilateration technique, estimating the next position of ED with a pre-defined trajectory. Apart from the existing enhanced ADR approaches, Semtech recommends blind ADR (BADR) to improve energy efficiency [13]. However, ADR, BADR, and existing enhanced ADR approaches are designed for one type of application at a time (e.g., either static or mobile) [5,14]. Therefore, to meet the diverse requirements of IoT applications, we propose a novel ADR called "hybrid ADR (HADR)" by allocating efficient resources (e.g., SF and TP) to static and mobile applications simultaneously.

The remaining of this paper is organized as follows: Section 2 presents the working of ADRs and discusses simulation results, and provides insights into the issues related to BADR and ADR. Section 3 presents the proposed HADR for static and mobile applications. Section 4 evaluates the proposed HADR in comparison with BADR and ADR. Finally, Section 5 presents some concluding remarks.

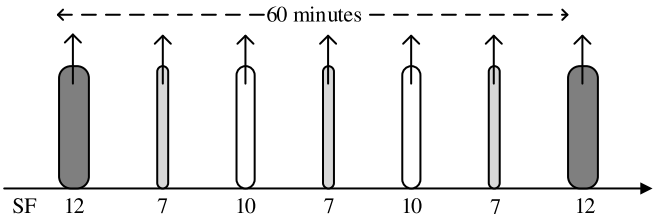

Fig. 3. Blind adaptive data rate at end device side.

2. Adaptive data rates in LoRaWAN

This section presents the typical ADR and blind ADR (BADR) variants, simulation analysis, and issues in these ADRs.

2.1. Adaptive data rate

Fig. 2 depicts the operation procedure of the NS side ADR, waiting for M packets prior to identifying new SF and TP parameters [6,11]. The new SF and TP identification is primarily based on the maximum signal-to-noise ratio (SNR_{max}) among M packets. The NS further computes the SNR required (SNR_{req}) for the current SF by taking the demodulation floor, SNR margin (SNR_{margin}) by subtracting the SNR_{max}, SNR_{req}, and $margin$. The minimum SNR_{req}, GW sensitivity (S_g), and ED sensitivity (S_e) required for demodulation at different SFs are listed in Table 1. Furthermore, the SNR_{margin} is an indicator used to judge whether the current SF of ED needs adjustment. While $steps$ defines the number of repetitions, ADR should be iterated to adjust both SF and TP. Finally, SF and TP parameters are sent to the ED via a DL MAC command $LinkAdrReq$.

2.2. Blind adaptive data rate

The SF assignment procedure of BADR is depicted in Fig. 3, where ED sends a packet with three SFs: SF 7 (three times), SF 10 (twice), and SF 12 (once) per hour [13].

2.3. Simulation analysis and issues with ADRs

We evaluate the ADR and BADR for mobile and static IoT applications in packet success and loss ratios (PSR and PLRs).

2.3.1. Application scenario

The BADR considers a GPS-based pet-tracking application in [13], where after every 10 min, the tracker wakes up and transmits a packet with a payload size of 13 bytes and GPS status of 17 bytes in the LoRa frame header (FHDR). To replicate this scenario, we have modified the optional MAC command of the FHDR to accommodate the ED positions, as shown in Fig. 4. Thus, the size of ED positions in our case is 8 bytes.

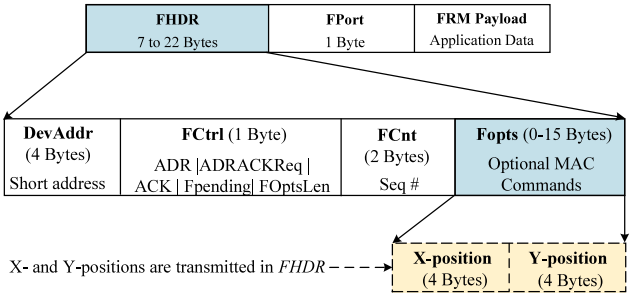

Fig. 4. Modified LoRa frame header.

2.3.2. Simulation setup

For the performance analysis of BADR and ADR, we utilize network simulator-3 (ns-3) by considering 100 EDs. These EDs employ log-distance and shadowing path loss models, where EDs are randomly deployed within a 6 km of radius around a single GW with an initial SF of 12 and TP of 14 dBm [7]. In addition, mobile EDs use Random Walk 2D mobility with a random speed between 2–4 m/s, as adapted in [5]. Both static and mobile ED transmit a UL packet every 10 min with a payload size of 30 bytes for a total simulation time of 24-h.

2.3.3. Analysis of ADR and BADR

The performance evaluation for the BADR and ADR under mobility and static conditions is presented in Figs. 5 and 6. As shown in Fig. 5, ADR under mobility conditions cannot adapt itself (in terms of SF and TP) due to the unstable channel environment, decreasing the PSR. In contrast, ADR in the static ED condition suffers from a significant convergence period, and then it could obtain a stable PSR by changing SF and TP. In contrast, the PSR of BADR in both underlying environments is constant. However, the PSR under mobility conditions is higher than that of static conditions. When an ED is not in the GW proximity owing to employing SF of 7 or 10, ED retransmits a packet with the same SF under a static scenario. However, in a mobility scenario, an ED moves around a GW; therefore, eventually, an ED can be in the GW proximity and can potentially retransmit that packet to the GW using SF of 7 or 10 successfully (allowed number of retransmission in the confirmed mode is 7). Generally, BADR in both cases outperforms the ADR under a static scenario in PSR.

In Fig. 6, the ratios for PSR and PLRs are shown. PLR-I (interference) is measured when packets have interfered with other packets. We consider both intra- and inter-SF interferences models as presented in [15,16]. It can be seen that ADR in static conditions suffers from interference due to the initial SF of 12 with high time-on-air (ToA). PLR-R (reception paths) arises when the receiving paths at the GW are busy during the reception of the incoming packets from the ED (8 receiving paths are considered in this work, which is based on [17]). However, the impact of PLR-R is negligible in a small number of EDs scenarios. It is because the GW in LoRaWAN is designed to receive 8 packets simultaneously.

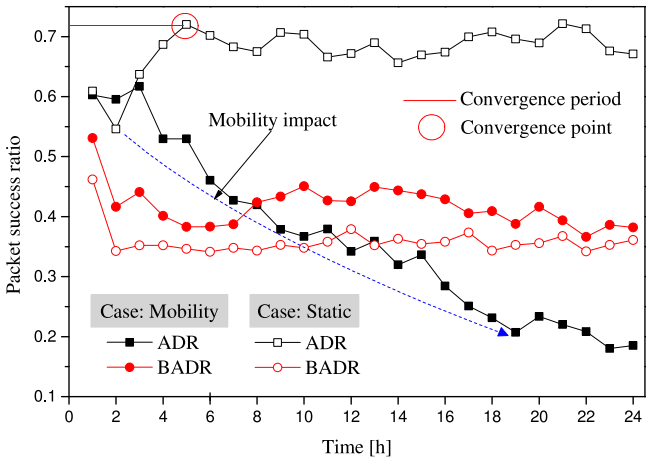

Fig. 5. Per-hour PSR of typical ADRs under mobile and static conditions.

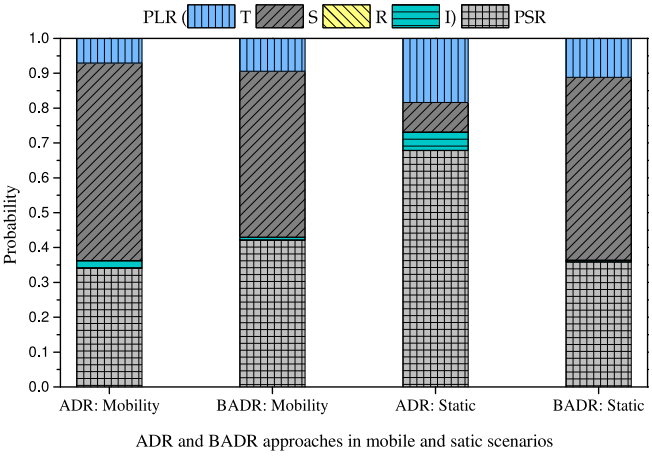

Fig. 6. Packet success and loss ratios of typical ADRs under mobile and static conditions.

PLR-S (sensitivity) happens when a packet reaches the GW under the required sensitivity. The impact of PLR-S is huge in ADR (mobile) and BADR (mobile and static) due to the inefficient use of SF, resulting in packets arriving under the required sensitivity thresholds. These sensitivity thresholds are defined in Table 1. Further, PLR-T (transmission) occurs due to the ACK transmission priority at the GW, when the collision occurs with ACKs [5]. In this work, we utilize bi-directional traffic, which causes PLR-T at the GW.

2.3.4. Issues with ADR and BADR

Based on the simulation analysis presented in this section, it is shown that both BADR and ADR are suffering from PLR-S. PLR-S is largely measured in ADR because of the ED movement, causing inappropriate SF and TP selection. BADR also does not consider the ED mobility in the SF allocation decision, resulting in a significant PLR-S when packets arrive under the SF sensitivity thresholds. However, its various SF selections make PLR-S reduced in the mobile ED scenario. In addition, Semtech [13] does not indicate a recommended use of SF in a retransmission mechanism since a packet can

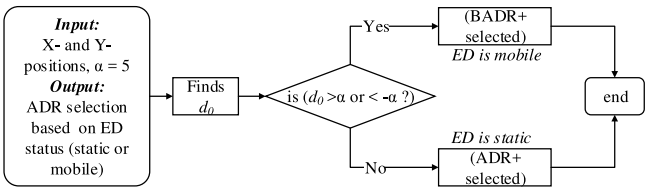

Fig. 7. Operation procedure of the proposed hybrid adaptive data rate.

be retransmitted seven times [the total number of allowed transmissions (Tx_{limit}) is set to 8] in a confirmed mode.

To resolve the issues mentioned above regarding the BADR and ADR, we propose a novel ADR called "hybrid adaptive data rate (HADR)". The proposed HADR is the extension of our conference paper [18], where we studied the feasibility analysis of BADR under a mobility scenario.

3. The proposed hybrid adaptive data rate

The operation procedure of the proposed HADR is shown in Fig. 7. There are two primary steps involved in the proposed HADR: computing the distance between previous and current locations of the ED (d_0) and ADR selection based on the ED status (i.e., static or mobile).

3.1. Computing d_0

HADR checks whether the ED is static or mobile at the time of each UL packet transmission. The d_0 is determined by finding the distance between the previous (x_1, y_1) and current (x_2, y_2) positions of an ED. We chose a threshold of $\alpha = 5$ m because the received signal strength remains unchanged up to 40 m [7].

3.2. ADR selection

Based on the d_0, HADR selects an appropriate ADR for the ED. When an ED is classified as mobile, BADR+ is initiated at the time of UL packet transmission (TX), as shown in Algorithm 1. The BADR+ is a slightly changed variant of BADR, where the ED transmits packets sequentially (i.e., [SF7∼SF12]). To resolve the retransmission issue of the BADR, we utilize a similar method, as shown in [15]. When ED fails to receive ACK, a retransmission counter ($ReTx\_CNT$) is incremented. If $ReTx\_CNT$ is a multiple of β (i.e., $\beta = 2$) SF is increased by 1 to regain connectivity [15].

In the case of static ED, the ADR+ manages both SF and TP, as shown in Algorithm 2. When NS receives M UL packets from the ED, the static ADR finds SF and TP based on the highest SNR value (SNR_{max}) among the M packets. However, we slightly modify the working of ADR by taking the moving average (SNR_{mAvg}) of M UL packets to smooth the SNR, which helps in identifying an efficient SF and TP. To find the best possible configuration of the SF and TP, the ADR+ computes the required SNR (SNR_{req}), SNR margin (SNR_{margin}), and $steps$. The $steps$ parameter defines the number of times the ADR should be iterated to adjust the SF and TP.

Algorithm 1: The proposed sequential BADR+ at the end device side.

Input : SF = 7∼ 12, $\beta = 2$, $TP = 14$ dBm
Output: Spreading factor and transmit power
Initiated at every UL packet transmission
if *(TX == True)* **then**
  `// starting SF = 7`
  Assign SF sequentially instead of [12, 10, 7])
else
  `// retransmission method`
  if *($ReTx\_CNT$ % β == 0 and SF < 12)* **then**
    SF = SF + 1
    TP = 14 dBm
  else
    continue transmission with current SF
  end
end

Algorithm 2: The proposed moving average-based ADR (ADR+) at the network server side.

Input : SF = 7∼ 12, TP = 2∼14 dBm, $M = 20$
Output: Spreading factor and transmit power
Initiated at every UL packet reception
if *(ACK == enabled)* **then**
  `// confirmed mode`
  1. SNR_mAvg = MovingAvg(SNR of last M UL packets)
  2. SNR_{req} = demodulation $floor$ (current DR/SF)
  3. SNR_{margin} = (SNR_m - SNR_{req} - $device_{margin}$)
  4. $steps = int$ (SNR_{margin}/3)
  while *($steps > 0$ and $SF > 7$)* **do**
    SF = SF - 1 and $steps = steps$ - 1
  end
  while *($steps > 0$ and $TP > 2$)* **do**
    TP = TP - 2 and $steps = steps$ - 1
  end
  while *($steps < 0$ and $TP < 14$)* **do**
    TP = TP + 2 and $steps = steps$ + 1
  end
end

4. Simulation analysis of the proposed HADR

The simulation settings are the same as utilized in Section 2 2.3.2. However, in the case of the HADR, EDs are assigned with SFs based on the GW sensitivities (during the initial deployment) to avoid interference occurring with SF12 owing to high ToA. These sensitivity thresholds are defined in Table 1.

4.1. Packet success ratio

Fig. 8 depicts the average PSR of the proposed HADR when compared with typical ADR and BADR approaches. In the mixed and static ED cases, ADR performs better than

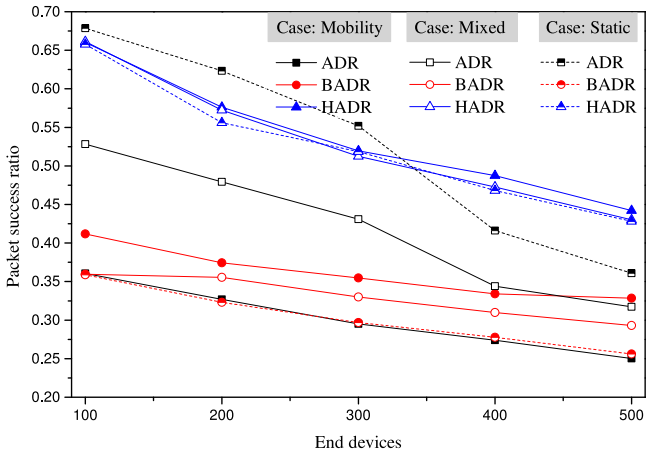

Fig. 8. PSR of the HADR, BADR, and ADR under different ED conditions.

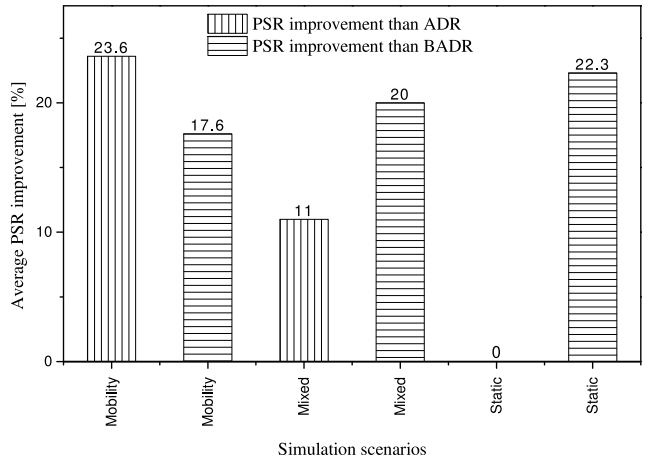

Fig. 9. PSR improvement in the proposed HADR.

BADR because of the low variations in the channel conditions. In contrast, BADR shows improved performance in the mobility scenario only by blindly transmitting with SF 12, 10, and 7. However, ED mobility affects the PSR of ADR. In the case of ADR, when a DL *LinkADRReq* MAC command with new SF and TP parameters arrives at the GW, the propagation environment surrounding the ED might be drastically affected. As a result, the parameters are no longer helpful since they may not successfully deliver a packet to the GW, leading to huge packet loss.

Compared to ADR and BADR, the proposed HADR performs significantly better by selecting the best SF using ADR+ for static EDs and blindly (without requiring prior knowledge, such as SNR or received power) transmitting with SF sequentially using the BADR+ for the mobile EDs. Thus, compared with typical ADR approaches, the proposed HADR enhanced the PSR, achieving its primary goal of PSR improvement in the mobility and mixed EDs scenarios, as shown in Fig. 9.

4.2. Packet loss ratios

Fig. 10 depicts the packet success and loss ratios under mixed scenarios (i.e., 50% of ED are static and 50% of the EDs are mobile). Generally, the ratios of PSR and PLRs equal one. Thus, the amount of sent or retransmitted packets contributes exclusively to either PSR or PLR. In Fig. 10(a), the ADR is primarily suffering from PLR-I and PLR-S, and PLR-T when the EDs increase. The PLR-I is caused due to high ToA when EDs transmit packets with SF of 12 during the initial deployment. When the NS adjusts the SF and TP based on the M packets, the ED might have moved to another position. Therefore, a packet transmitted with these new parameters arrives under the required threshold sensitivity at the GW, causing PLR-S. The PLR-T impact is approximately similar to all ADR approaches when the lost packets are retransmitted by ED (up to 7 times in the confirmed mode), increasing the network load in UL direction and causing a collision with ACK. In the case of BADR shown in Fig. 10(b), on average, 50% of the packets are lost owing to arriving under the required sensitivity threshold when transmitted with SF7 or SF10. Fig. 10(c) clearly shows that the proposed HADR resolves the issue of packets arriving under the required sensitivity by utilizing BADR+ and ADR+. Under a similar scenario, the final SF employed by the EDs is shown in Table 2.

4.3. Energy consumption

Fig. 11 shows an increase in energy consumption when the number of EDs is increased. The energy consumption of BADR is higher than ADR in the case of $N = 100$. When a packet is lost with SF of 12, it must be retransmitted with the same SF and TP of 14 dBm. Since higher energy consumption in LoRaWAN is primarily dependent on the SF, TP, ToA, and several retransmission attempts [7]. However, the energy consumption of ADR is lower than BADR under the same scenario. ADR at the NS side adjusts the SF and TP of the ED as soon as it receives M packets. When the number of EDs increases, the energy consumption is gradually increased in the case of ADR owing to interference caused due to high SF and retransmission, thereby reducing the network scalability.

HADR utilizes ADR+ for static and BADR+ for mobile EDs. In the case of ADR+, the SF and TP are adjusted by taking the moving average of the SNR of the M received packets at NS side, reducing the energy consumption. However, when mobile EDs utilize BADR+, a packet can be retransmitted several times (up to 7 times in the confirmed mode) if an ED is not in the GW proximity. In such a situation, the retransmission mechanism in the proposed BADR+ can increase the SF (when $SF < 12$) and allocate maximum allowed transmit power (i.e., TP = 14 dBm), at the cost of high energy consumption.

5. Conclusions

This paper presented a hybrid adaptive data rate (HADR) to simultaneously allocate resources (i.e., spreading factor and transmit power) to mobile and static EDs. Through simulation results, we observed that HADR performs better in PSR by using efficient SF and TP allocation, making it an ideal candidate for mobile and mixed types of EDs (static and mobile). Further, the ED part (BADR+) of the HADR can be applied to

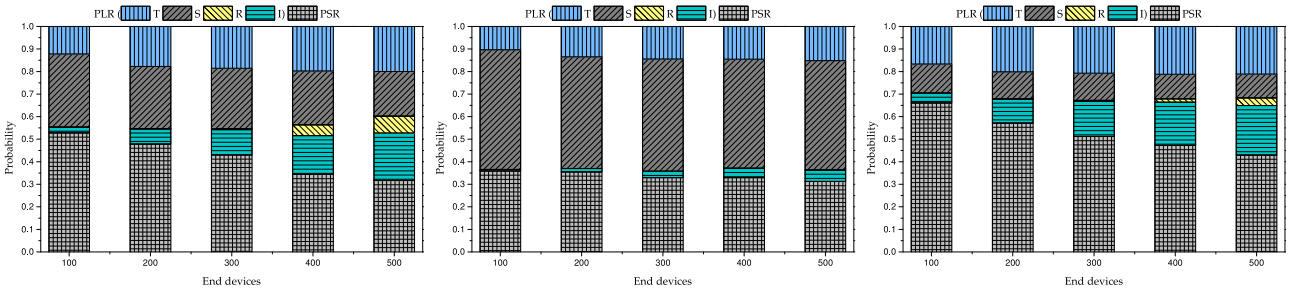

(a) ADR (b) BADR (c) HADR

Fig. 10. Packet success and loss ratios under mixed scenario (50% static and 50% mobile EDs).

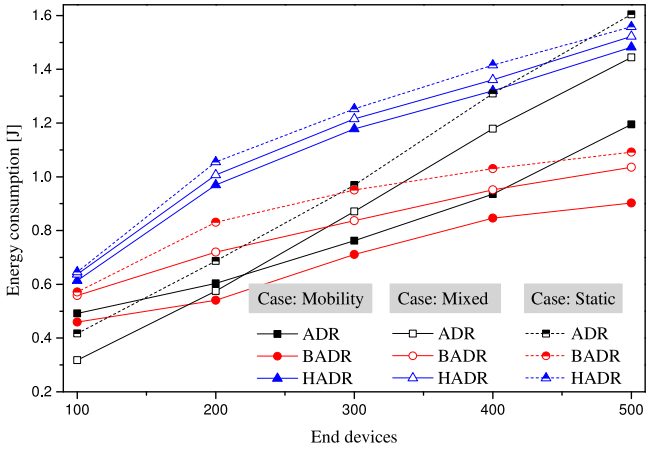

Fig. 11. Average energy consumption in [J].

Table 2
Final SF Utilization by the EDs in percentage for mixed end devices.

Approach	SF7	SF8	SF9	SF10	SF11	SF12
ADR	53.0	9.6	7.0	5.8	13.0	11.6
BADR	53.4	0	0	27.2	0	19.4
HADR	9.6	8.4	7.2	6.8	21.0	47.0

a realistic scenario by updating the firmware of the ED using "firmware update over the air". Conversely, the ADR+ of the proposed HADR at the NS can be easily integrated as part of routine maintenance.

CRediT authorship contribution statement

Arshad Farhad: Conceptualization, Methodology, Software, Data curation, Writing – original draft, Visualization, Investigation, Validation, Writing – review & editing. **Jae-Young Pyun:** Supervision, Project administration, Funding acquisition, Investigation, Validation, Writing – review & editing.

Declaration of competing interest

The authors declare that they have no known competing financial interests or personal relationships that could have appeared to influence the work reported in this paper.

Funding

This study was supported by research funds from Chosun University, Republic of Korea, 2021.

References

[1] G. Pasolini, On the LoRa chirp spread spectrum modulation. Signal properties and their impact on transmitter and receiver architectures, IEEE Trans. Wireless Commun. (2021) 1, http://dx.doi.org/10.1109/TWC.2021.3095667.

[2] K. Mekki, E. Bajic, F. Chaxel, F. Meyer, A comparative study of LPWAN technologies for large-scale IoT deployment, ICT Express 5 (1) (2019) 1–7.

[3] Q.-D. Ngo, H.-T. Nguyen, V.-H. Le, D.-H. Nguyen, A survey of IoT malware and detection methods based on static features, ICT Express 6 (4) (2020) 280–286.

[4] N.U. Okafor, Y. Alghorani, D.T. Delaney, Improving data quality of low-cost IoT sensors in environmental monitoring networks using data fusion and machine learning approach, ICT Express 6 (3) (2020) 220–228.

[5] A. Farhad, D.-H. Kim, J.-Y. Pyun, R-ARM: Retransmission-assisted resource management in LoRaWAN for the internet of things, IEEE Internet Things J. (2021) 1, http://dx.doi.org/10.1109/JIOT.2021.3111167.

[6] Semtech, Understanding the LoRa adaptive data rate, 2019, Technical Document URL https://lora-developers.semtech.com/uploads/documents/files/Understanding_LoRa_Adaptive_Data_Rate_Downloadable.pdf.

[7] A. Farhad, D.H. Kim, B.H. Kim, A.F.Y. Mohammed, J.Y. Pyun, Mobility-aware resource assignment to IoT applications in long-range wide area networks, IEEE Access 8 (2020) 186111–186124, http://dx.doi.org/10.1109/ACCESS.2020.3029575.

[8] J. Park, K. Park, H. Bae, C.-k. Kim, EARN: Enhanced ADR with coding rate adaptation in lorawan, IEEE Internet Things J. (2020).

[9] J. Finnegan, R. Farrell, S. Brown, Analysis and enhancement of the lorawan adaptive data rate scheme, IEEE Internet Things J. 7 (8) (2020) 7171–7180.

[10] A. Farhad, D.H. Kim, D. Kwon, J.Y. Pyun, An improved adaptive data rate for LoRaWAN networks, in: 2020 IEEE International Conference on Consumer Electronics - Asia (ICCE-Asia), 1-3 Nov. 2020, Seoul, Korea (South), 2020, pp. 1–4, http://dx.doi.org/10.1109/ICCE-Asia49877.2020.9276973.

[11] K. Anwar, T. Rahman, A. Zeb, Y. Saeed, M.A. Khan, I. Khan, S. Ahmad, A.E. Abdelgawad, M. Abdollahian, Improving the convergence period of adaptive data rate in a long range wide area network for the internet of things devices, Energies 14 (18) (2021) 5614.

[12] N. Benkahla, H. Tounsi, S. Ye-Qiong, M. Frikha, Enhanced ADR for LoRaWAN networks with mobility, in: 2019 15th International Wireless Communications & Mobile Computing Conference (IWCMC), Tangier, Morocco, 24-28 June, IEEE, 2019, pp. 1–6.

[13] Semtech, LoRaWAN mobile applications: Blind ADR, 2019, Technical Document URL https://lora-developers.semtech.com/library/tech-papers-and-guides/blind-adr/.

[14] A. Farhad, D.-H. Kim, S. Subedi, J.-Y. Pyun, Enhanced LoRaWAN adaptive data rate for mobile internet of things devices, Sensors 20 (22) (2020) 6466.

[15] A. Farhad, D.-H. Kim, J.-Y. Pyun, Resource allocation to massive internet of things in LoRaWANs, Sensors 20 (2645) (2020) 1–20.

[16] A. Farhad, D.-H. Kim, P. Sthapit, J.-Y. Pyun, Interference-aware spreading factor assignment scheme for the massive LoRaWAN network, in: 2019 International Conference on Electronics, Information, and Communication, ICEIC, IEEE, 2019, pp. 1–2.

[17] Semtech, Semtech SX1301 Wireless & Sensing Products datasheet, 2017, Technical Document URL https://www.semtech.com/products/wireless-rf/lora-gateways/sx1301.

[18] A. Farhad, D.-H. Kim, J.-S. Yoon, J.-Y. Pyun, Feasibility study of the LoRaWAN blind adaptive data rate, in: 2021 Twelfth International Conference on Ubiquitous and Future Networks, ICUFN, IEEE, 2021, pp. 67–69.